(2)

SECURITY CLASSIFICATION OF THIS PAGE

NTATION PAGE

1a. REPORT SECURITY CLASSIFICATION: UNCLASSIFIED	1b. RESTRICTIVE MARKINGS: DTIC FILE COPY
2a. SECURITY CLASSIFICATION AUTHORITY: AD-A201 440	3. DISTRIBUTION/AVAILABILITY OF REPORT: Approved for public release; distribution unlimited.
2b. DECLASSIFICATION/DOWNGRADING SCHEDULE: DEC 15 1988 S D CS	
4. PERFORMING ORGANIZATION REPORT NUMBER(S)	5. MONITORING ORGANIZATION REPORT NUMBER(S): AFOSR-TR- 88-1295
6a. NAME OF PERFORMING ORGANIZATION: HUGHES RESEARCH LAB	6b. OFFICE SYMBOL (If applicable):
6c. ADDRESS (City, State and ZIP Code): 3011 MAILBUSCANYON ROAD, MALIBU, CA 90265	7a. NAME OF MONITORING ORGANIZATION: AFOSR/NE
	7b. ADDRESS (City, State and ZIP Code): BLDG 410, BOLLING AFB, DC 20332-6448
8a. NAME OF FUNDING/SPONSORING ORGANIZATION: AFOSR	8b. OFFICE SYMBOL (If applicable): NE
	9. PROCUREMENT INSTRUMENT IDENTIFICATION NUMBER: F49620-87-C-0104
8c. ADDRESS (City, State and ZIP Code): Bldg 410, BOLLING AFB DC 20332-6448	10. SOURCE OF FUNDING NOS.

PROGRAM ELEMENT NO.	PROJECT NO.	TASK NO.	WORK UNIT NO.
61102F	DARPA	6140/00	

11. TITLE (Include Security Classification): DEVELOPMENT OF Si/SiGe HETEROSTRUCTURES

12. PERSONAL AUTHOR(S): Dr Hauenstein

13a. TYPE OF REPORT	13b. TIME COVERED	14. DATE OF REPORT (Yr., Mo., Day)	15. PAGE COUNT
Annual	FROM Sep 87 TO Sep 88		

16. SUPPLEMENTARY NOTATION

17. COSATI CODES			18. SUBJECT TERMS (Continue on reverse if necessary and identify by block number)
FIELD	GROUP	SUB. GR.	

19. ABSTRACT (Continue on reverse if necessary and identify by block number)

With the recent advances in Si molecular beam epitaxy (MBE) and limited-reaction processing (LRP), a viable, heterojunction-based device technology for Si may soon be at hand. Strained-Layer $Si_{1-x}Ge_x$ epitaxial alloy films and coherently strained $Si_{1-x}Ge_x/Si$ multilayer structures have been grown very successfully by MBE. More recently, high quality $Si/Si_{1-x}Ge_x/Si$ heterojunction bipolor transistors (HBT) having been fabricated by LRP techniques. $Si_{1-x}Ge_x/Si$ systems are of considerable interest because thcy provide Si-based semiconductor device technology with a pratical heterojunction capability which is also compatible with exiting device processing techniques. Semiconductors. GaAs

20. DISTRIBUTION/AVAILABILITY OF ABSTRACT	21. ABSTRACT SECURITY CLASSIFICATION
UNCLASSIFIED/UNLIMITED ☐ SAME AS RPT. ☐ OTIC USERS ☐	UNCLASSIFIED

22a. NAME OF RESPONSIBLE INDIVIDUAL	22b. TELEPHONE NUMBER (Include Area Code)	22c. OFFICE SYMBOL
LITTON	(202) 767-4931	NE

DD FORM 1473, 83 APR — EDITION OF 1 JAN 73 IS OBSOLETE.

SECURITY CLASSIFICATION OF THIS PAGE

1

HAC REF G3810

DEVELOPMENT OF Si/SiGe HETEROSTRUCTURES

R.J. Hauenstein

Hughes Research Laboratories
3011 Malibu Canyon Road
Malibu, California 90265

October 1988

Annual Report
September 1987 through September 1988

Sponsored by
Defense Advanced Research Projects Agency
DARPA Order No. 6140/00
Monitored by AFOSR Under Contract No. F49620-87-C-0104

DEPARTMENT OF THE AIR FORCE
Air Force Office of Scientific Research
Directorate of Electronic and Material Sciences
Building 410
Bolling AFB, DC 20332-6448

I. Introduction

With the recent advances in Si molecular beam epitaxy (MBE) and limited-reaction processing (LRP), a viable, heterojunction-based device technology for Si may soon be at hand. Strained-layer $Si_{1-x}Ge_x$ epitaxial alloy films and coherently strained $Si_{1-x}Ge_x/Si$ multilayer structures have been grown very successfully by MBE. More recently, high quality $Si/Si_{1-x}Ge_x/Si$ heterojunction bipolar transistors (HBT) having have been fabricated by LRP techniques. $Si_{1-x}Ge_x/Si$ systems are of considerable interest because they provide Si-based semiconductor device technology with a practical heterojunction capability which is also compatible with existing device processing techniques. The major impact of heterojunction device technology applied to Si is expected to be twofold: in the performance improvement of certain conventional Si devices such as the n-p-n bipolar transistor, and in the development within Si technology of novel device structures such as the High Electron-Mobility Transistor (HEMT).

For the n-p-n bipolar transistor, replacement of the base with a p-type $Si_{1-x}Ge_x$ alloy layer (i.e., the HBT) has already resulted in drastic improvement in transistor current gain performance, with β values as high as 400 being obtained. Moreover, projections for maximum high frequency operation of the conventional Si bipolar transistor, with the base width scaled down to 100Å, put f_T around 40GHz at best. In contrast, projections of 100GHz or better for f_T have been suggested for the $Si/Si_{1-x}Ge_x$ HBT, making this device a serious and probably superior alternative to the GaAs/AlGaAs HBT.

The performance advantages of the $Si/Si_{1-x}Ge_x$ HBT derive from the large (~100 meV) negative valence band offset ($\Delta E_V \equiv E_V^{Si} - E_V^{SiGe}$) at the emitter-base junction. The resultant large potential barrier presented to holes allow for a heavier base-layer and a lighter emitter-layer dopant concentration without sacrificing the large electron/hole minority carrier injection ratio needed for high current gain. Further, improved frequency performance is then possible because of the reduced series resistance in the more heavily doped base layer, and also a reduced base-emitter capacitance as the emitter need not be as heavily doped, both improvements leading to a reduced RC time constant. Thus, the physical properties of the $Si_{1-x}Ge_x/Si$ heterojunction are exploited to achieve something that is not possible in either material alone, and, in contrast with other materials systems, $Si_{1-x}Ge_x/Si$ heterojunction-based device structures are compatible with a mature and extensive Si device processing technology.

The approach and objectives of the present program are summarized in Fig. 1. Our goal is to fabricate four $Si_{1-x}Ge_x/Si$ heterojunction devices: the heterojunction diode, the HEMT, the high hole mobility transistor (HHMT), and the HBT. Of these, the HBT is the most likely to have major technological significance in the near term. Accordingly, we wish to focus our efforts on development of the HBT. As indicated in Fig. 1, our approach is conceptually structured as follows: (1) get the materials problems under control; (2) get the doping under control; (3) fabricate and characterize prototype device structures; (4) to the extent possible here, work toward device optimization.

To this point, we have been mainly involved with establishing the growth conditions which optimize the structural quality of $Si/Si_{1-x}Ge_x/Si$ heterostructures. As indicated in Fig. 1, MBE is the epitaxial growth technique being employed in this work. Unfortunately, our MBE machine

was not delivered until Feb 88 (five months into this contract). Nevertheless, despite this late start as well as subsequent problems with the MBE machine, we have been able to produce state-of-the-art multilayered structures within three months. Meanwhile, Perkin-Elmer has grown a set of four HBT structures for us. These four structures, in addition to two HBT structures grown in the HRL system, have been extensively characterized structurally through cross-sectional transverse electron microscopy (TEM), Auger depth profile, and high-resolution x-ray diffraction (HRXRD) measurements. We have succeeded in establishing the growth conditions necessary to produce high quality, coherently strained epitaxial structures. At this point, we have just now begun to consider electrical characteristics and doping, including both unintentional background doping from the MBE system, and the control of intentional dopant profiles. The remainder of this report is organized as follows: First, we will discuss the importance of strain effects in lattice-mismatched $Si_{1-x}Ge_x/Si$ structures. After this will be a brief section summarizing the experimental details of the samples being reported on here. Next we will discuss the results of structural characterization of our six $Si/Si_{1-x}Ge_x/Si$ HBT structures. Following this will be the results of our preliminary doping experiments and electrical characterization of nominally undoped structures. Then, we will mention the other Si MBE activities at HRL which are running concurrently with the present contract. Finally, we will summarize our technical results to the present time, and outline the future direction of this program.

II. Strain Effects and Critical Thickness in $Si_{1-x}Ge_x/Si$

In electronic devices based on $Si_{1-x}Ge_x/Si$ heterostructures, the physical and materials concerns of greatest importance are the following: (1) the "bulk" band structures of individual layers, (2) the band offsets between layers, (3) the structural quality of layers and interfaces, (4) the control of compositional and dopant profiles, and (5) the effects of strain. In any heteroepitaxial materials system, the first four of these items must be controlled, or at least understood, in order to successfully produce device structures. However, because of the large (4.2%) lattice-constant mismatch between Si and Ge, strain plays a particularly important role in the $Si_{1-x}Ge_x/Si$ system, a role much more critical here than in lattice-matched systems such as GaAs/AlAs. The lattice mismatch at a $Si_{1-x}Ge_x/Si$ interface must be accommodated in one of two ways (or a combination thereof): through the formation of misfit dislocations, or through elastic distortion (strain). The particular mode of misfit accommodation can be expected to significantly alter device performance as we now discuss.

Interfacial dislocations at heterojunction interfaces are generally undesirable as they give rise to leakage currents in devices depending on charge transport across the junction (such as the HBT), and result in a mobility reduction in HEMT-like device structures. On the other hand, elastic strain modifies both bandstructure and band offset. For example, the sign of the $Si_{1-x}Ge_x/Si$ conduction band offset ΔE_c is strain-dependent for certain compositions while ΔE_v is always of the same sign, making possible both type-I and type-II band alignments. Also, strain effects can remove energy degeneracies among conduction or valence band extrema. The maximum thickness of a $Si_{1-x}Ge_x$ layer grown on a Si substrate that is still coherently strained is known as the **critical thickness**. The experimentally observed critical thickness is a very strong function of the lattice mismatch (hence alloy composition x), and also depends on the growth temperature and the detailed epitaxial structure. Layers grown thicker than the critical thickness exhibit misfit dislocations and reduced and inhomogeneous strain.

Strain effects may be exploited. For instance, in the ideal HBT structure grown on (100)-Si, assuming a Si-like conduction band structure with six equivalent Δ-direction minima (valid for compositions $x < 0.85$), the coherent base-layer strain (an in-plane biaxial compression accompanied by an extension along the interface normal) raises the energy of the two minima aligned along the interface normal while lowering that of the other four minima. This results in a lower effective mass component for transport normal to the interface, and the partial removal of intervalley phonon scattering, both of which enhance the electron mobility across the heterojunction. Another example concerns the HEMT structure coherently strained to a thick $Si_{1-x}Ge_x$ buffer-layer lattice constant. In this case ΔE_c can be made negative, resulting in two-dimensional electron confinement on the Si rather than the $Si_{1-x}Ge_x$ side of the interface, thereby eliminating alloy scattering mechanisms. In addition, the strain in this case is opposite to that described above for the HBT, resulting this time in an in-plane electron mobility enhancement in the HEMT (for similar reasons to those cited above for the HBT). Clearly, strain plays an important role in determining the electronic properties of $Si_{1-x}Ge_x$/Si heteroepitaxial structures.

III. Growth Procedure

Here we describe the growth procedure which was used to prepare the two HRL-grown HBT samples. A similar procedure was used by Perkin-Elmer to grow the four earlier specimens. Our films were grown on wafers prepared through a solvent degrease procedure followed by an HF dip and deionized water rinse immediately prior to loading into the chamber.

The growth surfaces were prepared in situ by heating the wafers to 850 to 900°C in the presence of a low Si flux. The wafers were then cooled to the starting growth temperature (~750°C) and a Si layer (serving as both buffer and the "collector") was grown, during which the growth temperature was continuously ramped down to 390°C. The $Si_{1-x}Ge_x$ "base" and Si "emitter" layers were then grown at 390°C. Temperatures were assessed by means of an optical pyrometer, calibrated through observation of the Si:Al eutectic reaction, and feedback-stabilized temperature control was effected by means of a thermocouple which was also calibrated against the optical pyrometer. Nominal deposition rates were near 1Å/sec for the Si, along with the Ge rate required to produce the desired $Si_{1-x}Ge_x$ compositions in the base layer. All layers were nominally undoped although electrochemical C-V profile (CVP) and spreading resistance (SRP) analyses revealed the presence of an n-type dopant at a concentration on the order of 10^{15} cm^{-3}. This will be discussed further in Section V below.

The characteristics of our six HBT structures are summarized in Table I. (The two samples whose ID's contain the prefix "HA" were grown in the HRL Si MBE chamber; the remaining four were grown in the Perkin-Elmer Si MBE prototype chamber by Dr. Peter Cho.) Initially, four HBT structures (nominally 5000 Å Si / 1500 Å $Si_{1-x}Ge_x$ / 2500 Å Si) were grown by Perkin-Elmer. Two of these structures were grown on a substrate held at 390°C (samples #87.109 and 88.009), and two were grown at 530°C (samples #88.002 and 88.010). Fractional Ge concentrations in the base layers of x = 15% and x = 30% at each growth temperature were attempted. Similar structures were attempted in our (at that point uncalibrated) system.

IV. Structural Characterization of Si/$Si_{1-x}Ge_x$/Si Multilayers

In this section, we report the results of structural characterization of a set of six $Si/Si_{1-x}Ge_x/Si$ HBT structures. The HBT structure is indicated schematically in Fig. 2. Our samples have been characterized through cross-sectional TEM, HRXRD, and Auger profile measurements. The purpose of the present experiments is to establish the optimum growth conditions which lead to high quality, coherently strained growth. In particular, growth temperature and $Si_{1-x}Ge_x$ alloy layer composition (x) were varied to determine if above-critical-thickness growth of coherently strained HBT structures is possible.

Previous work[1] on $Si/Si_{1-x}Ge_x$ strained-layer superlattices has shown that, for those structures, coherently strained films with thicknesses in excess of the "critical thickness" can be metastably grown at sufficiently low growth temperatures, and that the onset of strain relaxation in the superlattices was temperature dependent, suggesting a kinetic barrier to misfit dislocation formation. Here, we seek to discover if a similar phenomenon exists and can be exploited for the HBT structure. For the HBT device, a coherently strained structure (free of misfit dislocations at the heterojunction interfaces and free of threading dislocations throughout the device structure) is important for achieving the desired band offset with minimum leakage at the emitter-base junction, and hence, the maximimum current gain performance.

Figures 3 and 4 show cross-sectional TEM images of the four Perkin-Elmer samples. Auger profile analysis reveals that the actual base layer compositions (ranging from x = 14% to 42%) varied substantially from the intended values of x = 15% and 30%. A typical Auger depth profile, taken at the HRL surface analytical laboratory, is shown in Fig. 3. The TEM images of

1. R. H. Miles, P. P. Chow, D. C. Johnson, R. J. Hauenstein, C. W. Nieh, and M. D. Strathman, Appl. Phys. Lett. 52, 916 (1988).

the four Perkin-Elmer samples are shown ordered from highest (x = 42%) to lowest (x = 14%) alloy layer Ge concentration (from Figs. 4(a)--5(b).) The base thicknesses of all four samples are nominally 1500Å; actual thicknesses, as well as the critical thickness from People and Bean's curve[2] for the given actual base layer composition, are shown in Table I. From the table we see that the actual thickness of sample #87.109 (1300Å) is considerably in excess of Bean's critical thickness for this composition (200Å). Indeed, Fig. 4(a) shows that sample #87.109 is quite relaxed, and clearly shows the presence of a high density of stacking faults and some microtwins. Also apparent are ripples of strain contrast in the $Si_{1-x}Ge_x$ layer as well as the appearance of an interfacially localized dislocation network at the collector-base interface. TEM data acquired with the specimen slightly tilted (not shown) shows quite clearly the presence of an interfacial network of misfit dislocations. This indicates that the base layer has relaxed to an average lattice constant larger than that of Si, forcing the Si emitter overlayer itself to re-relax back to the Si lattice constant value. The degradation of the emitter (top Si) layer crystalline quality due to the large and inhomogenous strain in the base layer, and high density of stacking faults threading through the base-emitter interface, is readily apparent in Fig. 4(a). There we see that the upper half of the emitter layer contains a very high density of microtwins and the upper surface of the film is quite rough (~100Å).

Figure 4(b) shows that sample #88.010 is also partially relaxed, as is evidenced by the fringes of strain contrast in the base layer, particularly near the interfaces, and also in the Si collector layer below. Weak-beam dark field TEM with the specimen slightly tilted shows the presence of a misfit dislocation network at both the collector-base and base-emitter interfaces, and also reveals threading dislocations in the base and emitter layers. Comparing Fig. 4(b) with

2. R. People and J. C. Bean, Appl. Phys. Lett. 49, 229 (1986).

Fig. 4(a), we see that the former is not as completely relaxed, and is obviously of better crystalline quality than the latter. This is probably because of the smaller ratio of actual to critical thicknesses in the former case, as well as the higher growth temperature (530 $^{\circ}$C) used for sample #88.010.

The crystalline quality is much improved as composition and thickness are adjusted to satisfy the People and Bean critical thickness curve as judged from the TEM photographs pictured in Fig. 5. First, in Fig. 5(a) we see pictured a cross section of sample #88.002, which shows a much more uniform, largely dislocation-free structure with abrupt, planar interfaces. We do not observe any threading or interfacial misfit dislocations in this specimen, but do see some strain-induced contrast in the structure. The coherently strained base layer is even more apparent in Fig. 5(b), the only specimen of the four Perkin-Elmer samples to exhibit a fully coherently strained structure. Sample 88.009 is also the only Perkin-Elmer specimen whose thickness and composition satisfy the condition for a coherently strained structure; i.e., $t < t_c(x)$, where $t_c(x)$ is the People and Bean critical thickness of a $Si_{1-x}Ge_x$ alloy on Si. Also seen in Fig. 5(b) are unusual microscopic cracks extending down from the film surface. We do not understand the significance of these cracks at present; in particular, they may be artifacts of the TEM specimen preparation.

Figure 6 shows a TEM cross-section of the first of our two HRL-grown HBT structures (sample #HA88.006). In terms of crystalline quality, it appears that sample #HA88.006 is the best of the six samples studied. From the figure, we see perfectly abrupt, planar interfaces, the complete absence of any dislocations, and extremely uniform contrast within each of the epilayers, indicative of a nearly ideal, coherently strained structure. As seen in Table I, this

sample is evidently just at the critical thickness limit. Finally, no TEM data is available for our other HRL-grown sample, HA88.007, which we know to be relaxed (as expected from the composition and thickness) from high resolution x-ray diffraction data, as we now discuss.

All of the HBT structures have been structurally characterized with the use of HRXRD. Our measurement system involves the use of a four-crystal monochromator and a stationary, large-acceptance-angle detector set up to detect the symmetric Bragg reflection of the (400) Si and $Si_{1-x}Ge_x$ alloy peaks. The four-crystal monochromator provides extremely monochromatic (5 arc sec) Cu-Kα_1 radiation which enables accurate assessment of diffraction peak widths. The peak widths are dependent upon the thickness and crystalline quality of an epilayer. Sharp x-ray peaks are indicative of flat, uniformly strained layers free from extended structural defects (dislocations and stacking faults). These peaks become broadened by the presence of extended defects, microscopic roughness, and spatial inhomogeneity of residual stresses. Such residual stresses are present near interfaces of lattice-mismatched $Si/Si_{1-x}Ge_x$ layers when the materials are not coherently strained. Since HRXRD is much less time-consuming and sample-preparation intensive than is TEM, it is desirable to interpret our HRXRD results with reference to the TEM.

Figures 7(a) and 7(b) show a pair of HRXRD spectra taken for two representative HBT structures, one having a coherently strained and the other an incommensurate (relaxed) $Si_{1-x}Ge_x$ layer. These correspond to the TEM photos shown in Figs. 5(b) and 4(a). The coherently strained sample (Fig. 7(a)) produces an extremely sharp $Si_{1-x}Ge_x$ (400) peak, shifted due to biaxial strain, whose peak width is due to the finite size (~1200Å) of the layer. Earlier, we saw from Fig. 5(b) that this sample has a base layer which is uniformly strained and free of threading

dislocations, and possesses abrupt, planar interfaces without misfit dislocations. In contrast, Fig. 7(b) contains a broad, weak alloy peak. Referring to Fig. 4(a), we see that this structure is quite relaxed and heavily dislocated, as noted above. The peak position and lineshape of the sample with the sharpest $Si_{1-x}Ge_x$ peak (88.009) correspond to the sample which is coherently strained and of high crystalline quality. As strain relaxation proceeds, we observe a systematic weakening and broadening of our x-ray peaks. Indeed, the most completely relaxed sample (87.109) exhibits the weakest and broadest $Si_{1-x}Ge_x$ x-ray peak.

On examining the set of four HBT samples grown by Perkin-Elmer, plus the two samples grown by ourselves at HRL, we find that the critical thickness marking the onset of strain relaxation and misfit defect formation is in agreement with established critical thickness results for single $Si_{1-x}Ge_x$ layers on Si, despite the fact that some of our samples have been grown at temperatures as low as 390°C. This is seen in Table II, where we compute the "% relaxation" for each sample, based on the Auger-determined $Si_{1-x}Ge_x$ composition and the peak position of the alloy layer (400) x-ray peak. To within experimental error, all samples in excess of the critical thickness exhibit some degree of strain relaxation except for sample #88.009, which has $t < t_c$. The excellent TEM results shown in Fig. 6 on the HRL sample suggests that this structure is also nearly perfectly coherently strained, in apparent disagreement with the x-ray results, which qualitatively indicate a sharp alloy peak, but a peak position consistent with a partially (32%) relaxed structure. This discrepancy may be due to an error in the measurement of $Si_{1-x}Ge_x$ layer composition. For example, an actual composition of $x = 22\%$ instead of the measured 25% would resolve the discrepancy, and would put this sample below the critical thickness curve. More generally, the correlation between our x-ray and TEM results show the utility of HRXRD in indicating the presence of microstructural imperfection. What remains is to extract

quantitative information about defect density from the width of the x-ray peaks. This becomes ambiguous in the case of a very broad x-ray peak due to the multiplicity of possible broadening mechanisms. Fortunately, HRXRD is directly useful for the immediate identification of high quality samples, and in this case, quantitative analysis of the peak-width information is possible.

Finally, we fail to observe any significant effect of the growth temperature on the "critical thickness," i.e., on the onset of strain relaxation, in our HBT structures. This finding is in contrast with the results reported for $Si_{1-x}Ge_x/Si$ strained-layer superlattices, where the alternating strain fields present in the strained-layer superlattice structure may play a role in slowing the kinetics of strain relaxation. Hence, our results to this point suggest that the critical thickness data deduced by People and Bean are appropriate guidelines in the design of HBT structures grown at temperatures between 390 and 530 °C.

V. Doping and Electrical Characterization of $Si/Si_{1-x}Ge_x/Si$ Multilayers

As noted above, our six HBT samples were all nominally undoped. In order to characterize the background of unintentional dopants from our Si MBE machine during growth, we have made various measurements, including spreading resistance profiling (SRP), electrochemical capacitance-voltage profiling (CVP), secondary-ion mass spectroscopy (SIMS), and photoluminescence (PL) measurements. A typical background dopant profile for an "undoped" sample is shown in Fig. 8. We see that the majority background dopant is n-type in the 10^{15} cm^{-3} range. Attempts to identify the dopant species through PL or SIMS have proven unsuccessful; however, the dopant is believed to be phosphorous. This is characteristic of new

Si MBE systems. The suspected source is outdiffusion of phosphorous from the stainless steel chamber walls. With use of the MBE, the phosphorous level is expected to decrease to a point where it is typically replaced by boron as the predominant background dopant. The ultimate background in used systems appears to be in the high 10^{13} cm^{-3} to low 10^{14} cm^{-3} range. We mention here that not enough is known about contamination levels from deep level impurities; in particular, it may be these that ultimately limit the performance of HBT structures produced by MBE (vs. LRP).

We have just recently begun our first deliberate attempts at doping. Perkin-Elmer has grown a set of samples in which boron and antimony fluxes were produced from effusion sources in their Si MBE prototype chamber. Figure 9 shows a boron dopant profile in a Si epilayer on a Si substrate, measured by SRP. In this case, elemental boron was used as the dopant source. A staircase profile was attempted (each step of 1000Å thickness). The SRP measurement could not resolve the steps. However, from the figure we see activation at concentrations up to 10^{20} cm^{-3}, with no adverse effect on film morphology, or, evidently, on crystalline quality. We are presently making SIMS measurements on this sample to determine the activation efficiency, and to attempt to spatially resolve the steps designed into the dopant profile.

Similar initial attempts at doping with antimony have proven less successful. In particular, Perkin-Elmer applied a negative bias voltage to the substrate during deposition/doping in an effort to exploit the potential-enhanced doping (PED) effect. However, the results at this point are inconclusive; further samples are already being grown.

Finally, we point out that our own Si MBE system has been loaded with Ga (p-type) and Sb (n-type) dopant materials. These will be effusion-cell codeposited during e-beam deposition of the Si and Ge primary materials. We hope to begin fabricating samples by mid-October in the HRL system.

VI. Concurrent Si MBE Activities at HRL

At this point, we would like to briefly mention other Si MBE-related efforts taking place concurrently with the present program. First, HRL has a contract with AFOSR/DARPA for the development of Si:Ga impurity-band conduction extrinsic detectors. This Si:Ga program will end at about the same time as the present program. Next, we have been pursuing several related activities under internal research and development (IR&D) funding. During the past year, these efforts have included: collaboration with Caltech (R. H. Miles and T. C. McGill) and Perkin-Elmer (P. P. Chow) to study the dependence of lattice mismatch accommodation on growth temperature in $Si_{1-x}Ge_x/Si$ strained-layer superlattices; development of in-house characterization techniques (used by all of our Si MBE programs) such as HRXRD, and development of computer simulation programs to analyze strain, layer thicknesses, and composition in $Si_{1-x}Ge_x/Si$ multilayered structures; investigations of the kinetics of strain relaxation in $Si_{1-x}Ge_x/Si$ heterostructures such as superlattices and single layers through x-ray and Raman scattering techniques. In particular, as a demonstration of our material fabrication and characterization capabilities, we have grown strained-layer superlattices which have been shown to be of state-of-the-art material quality, as verified by cross-sectional TEM and lattice-imaging, HRXRD, and improved resolution Auger profile measurments. We have obtained

excellent agreement between our experimental HRXRD and computer simulated spectra with respect to superlattice peak positions, intensities, and widths, indicating microstructural perfection over over macroscopic distances, and good compositional and thickness uniformity throughout the superlattice. Also, our surface analytical laboratory has been able to spatially resolve Auger compositional profiles for superlattice $Si_{1-x}Ge_x$ layers as thin as 38Å through substrate rotation techniques.

VII. Summary

In summary, despite a late delivery of our Si MBE equipment, we have produced the first epitaxial films in our MBE system within three months. Characterization of these films has shown them to be of comparable structural quality to state-of-the-art Si MBE films, provided that the appropriate growth conditions are chosen. Our efforts to this point have focused on materials properties of $Si_{1-x}Ge_x$/Si heterostructures; particularly, on the HBT device structure, with an emphasis on establishing the growth conditions needed to achieve reliable, high quality growth. In this report, we considered the effect of substrate growth temperature on strain relaxation in $Si_{1-x}Ge_x$/Si HBT structures. We have found that the critical thickness curves experimentally determined by People and Bean for single $Si_{1-x}Ge_x$ layers on Si represent appropriate guidelines for the %Ge content and thickness of the $Si_{1-x}Ge_x$ base of the HBT structure; no significant dependence of the critical thickness on growth temperature was observed among the samples studied here. Our TEM results suggest that it should be possible to grow high quality, dislocation-free, coherently strained HBT structures at temperatures ranging between 390 and 530 °C, provided that the base thickness does not exceed t_c given by People and Bean.

At present, initial attempts to develop and optimize epilayer doping techniques are underway. In particular, we believe it to be very important to the success of electronic materials produced by Si MBE to better understand and control the nature of leakage-causing defects and deep levels in devices which make use of a p-n junction. Other techniques such as LRP have fabricated superior $Si_{1-x}Ge_x$/Si HBT devices. This success is possibly due to superior material purity with respect to the presence of deep-level states in the base-emitter junction. As of yet, there is no evidence to expect that there is any fundamental reason why a Si molecular beam process cannot provide acceptable material quality while retaining the flexibility and all the other comparative advantages that the molecular beam approach has to offer. Finally, we soon expect to be at the point of fabricating prototype p-n heterojunction diode and n-p-n HBT structures for characterization and analysis.

Table I

Sample	T_g(°C)	x_{nom}(%)	x_{act}(%)	t_{TEM}(Å)	t_c(Å)
87.109	390	30	42	1300	200
88.010	390	30	26	1700	900
88.002	530	15	25	1650	1000
88.009	530	15	14	1200	4000
HA88.006	390	15	25	1050	1000
HA88.007	390	30	35	-	400

Table II

Sample	% Relaxed
87.109	-5 (±15) %
88.002	22 (±10) %
HA88.006	32 (±10) %
88.010	28 (±10) %
HA88.007	47 (±5) %
87.109	84 (±5) %

Figure Captions

Figure 1 Conceptional diagram showing organization and goals of the HRL SiGe/Si Heterostructures program.

Figure 2 Schematic of the HBT structure. The thicknesses and dopant concentrations shown differ from those of the samples reported here.

Figure 3 Typical Auger depth profile of an HBT structure.

Figure 4 Cross-sectional TEM of Perkin-Elmer-grown sample (a) 87.109; (b) 88.010. The structure is Si/$Si_{1-x}Ge_x$/Si on a Si-(100) substrate.

Figure 5 Cross-sectional TEM of sample (a) 88.002; (b) 88.009. The structure is Si/$Si_{1-x}Ge_x$/Si on a Si-(100) substrate.

Figure 6 Cross-sectional TEM of HRL-grown sample HA88.006. The dark band is the $Si_{1-x}Ge_x$ layer. The structure is Si/$Si_{1-x}Ge_x$/Si on a Si-(100) substrate.

Figure 7 High-resolution x-ray diffraction scans of sample (a) 88.009; (b) 87.109. The large, truncated peak is the (400)-Si reflection from the substrate, and the small peak is due to the $Si_{1-x}Ge_x$ layer. Note the difference in peak widths, due to differences in microstructural crystalline quality of the alloy layer.

Figure 8 Spreading resistance profile of a nominally undoped sample (HA88.007). The epilayer profile is due to n-type background doping from the Si MBE chamber.

Figure 9 Spreading resistance profile of a sample intentionally doped with boron.

HRL SiGe/Si HETEROSTURCTURES PROGRAM OVERVIEW

HUGHES

C18051-1

- DEVICE GOALS: { HJ DIODE
  HEMT, HHMT
  (HBT)
- APPROACH:

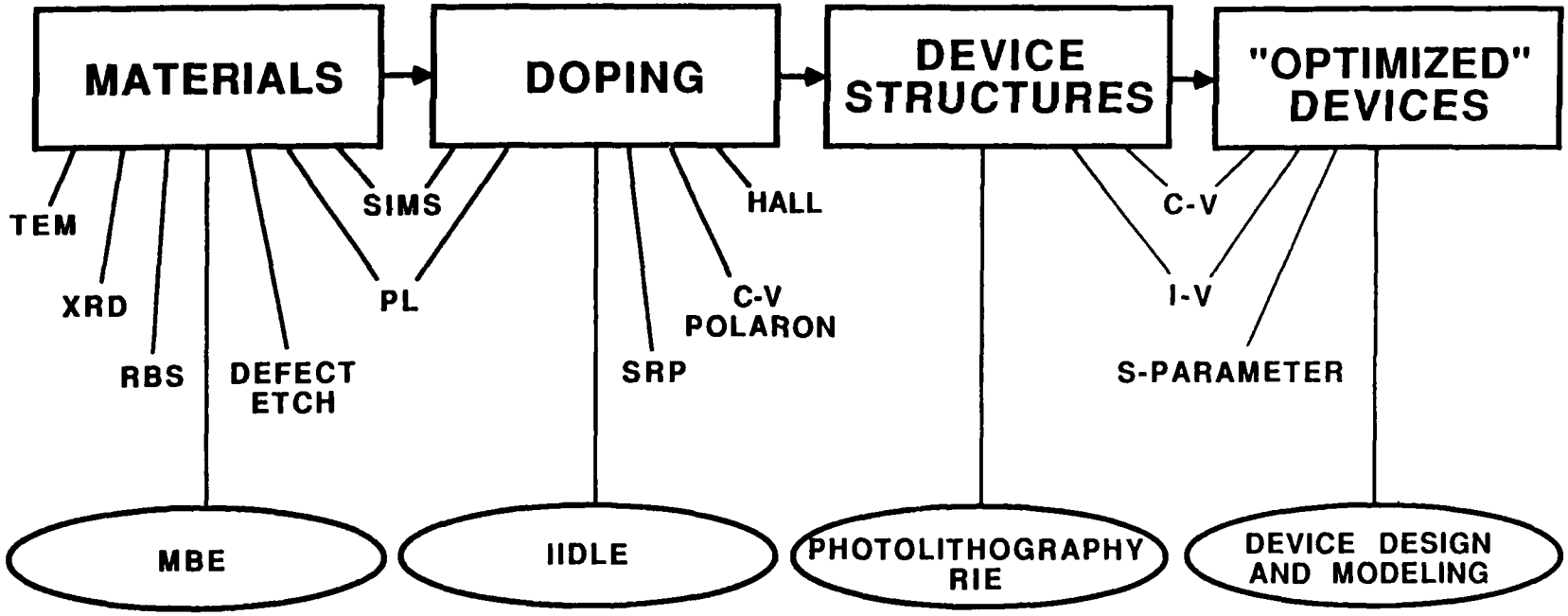

MARCH 1988

FIG. 1

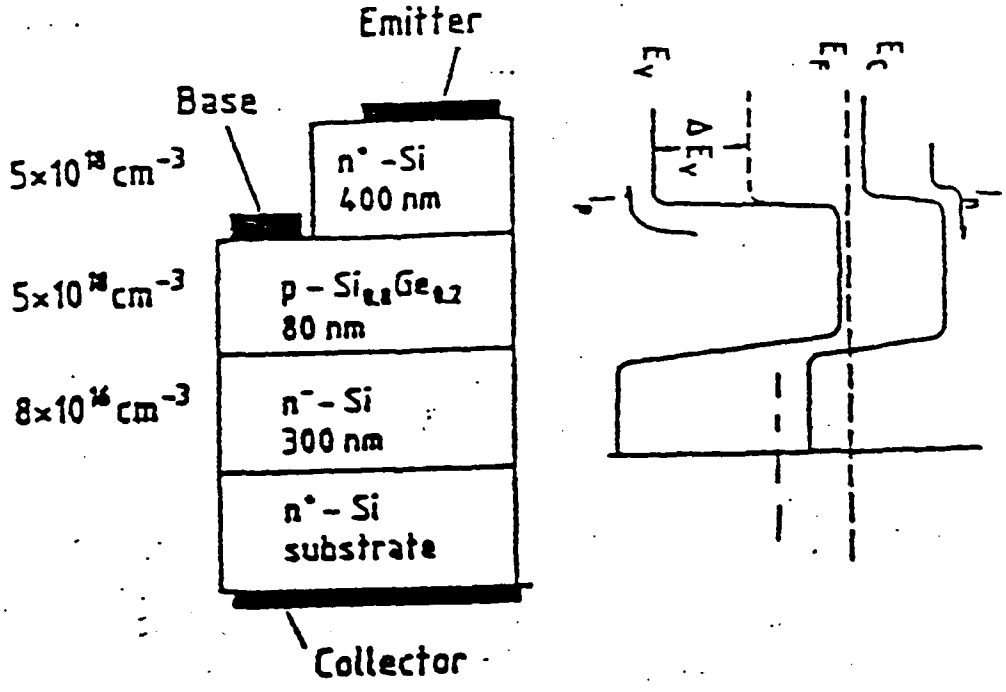

Fig. 12: Hetero bipolar structure
1307

*H. Daembkes, in *Proc. of the 2nd International Symposium on Silicon Molecular Beam Epitaxy*, ed. by John C. Bean and Leo J. Schowalter (The Electrochemical Society, Pennington), 1988, p. 15.

HAUENSTEIN

FIG. 2

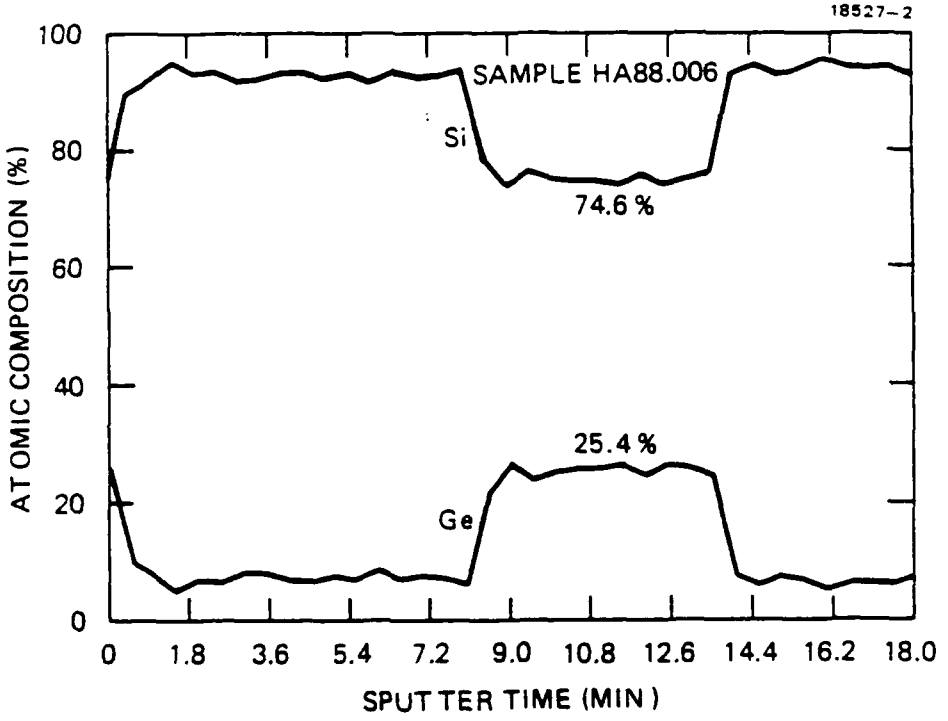

HAUENSTEIN
FIG. 3

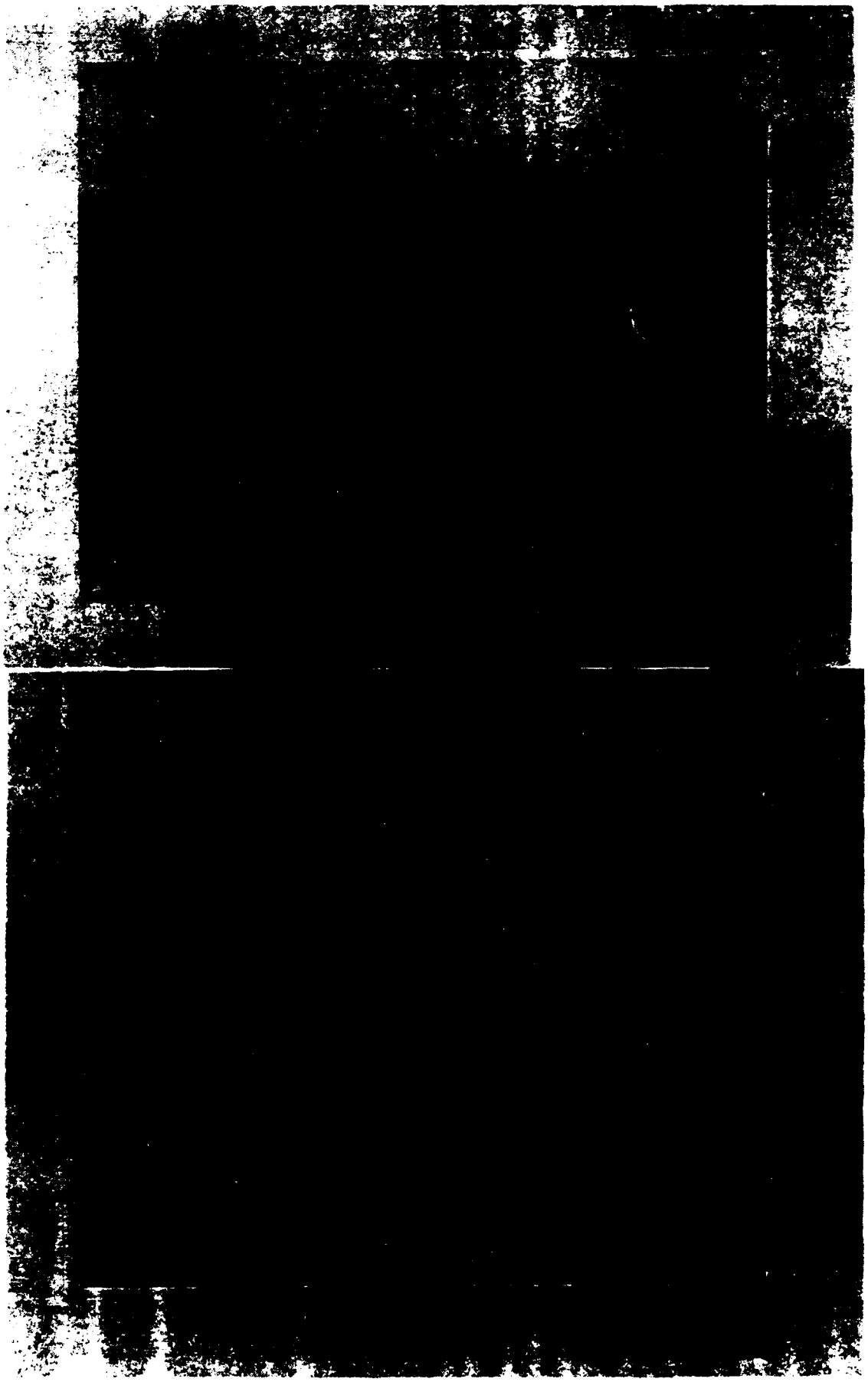

FIG. 4

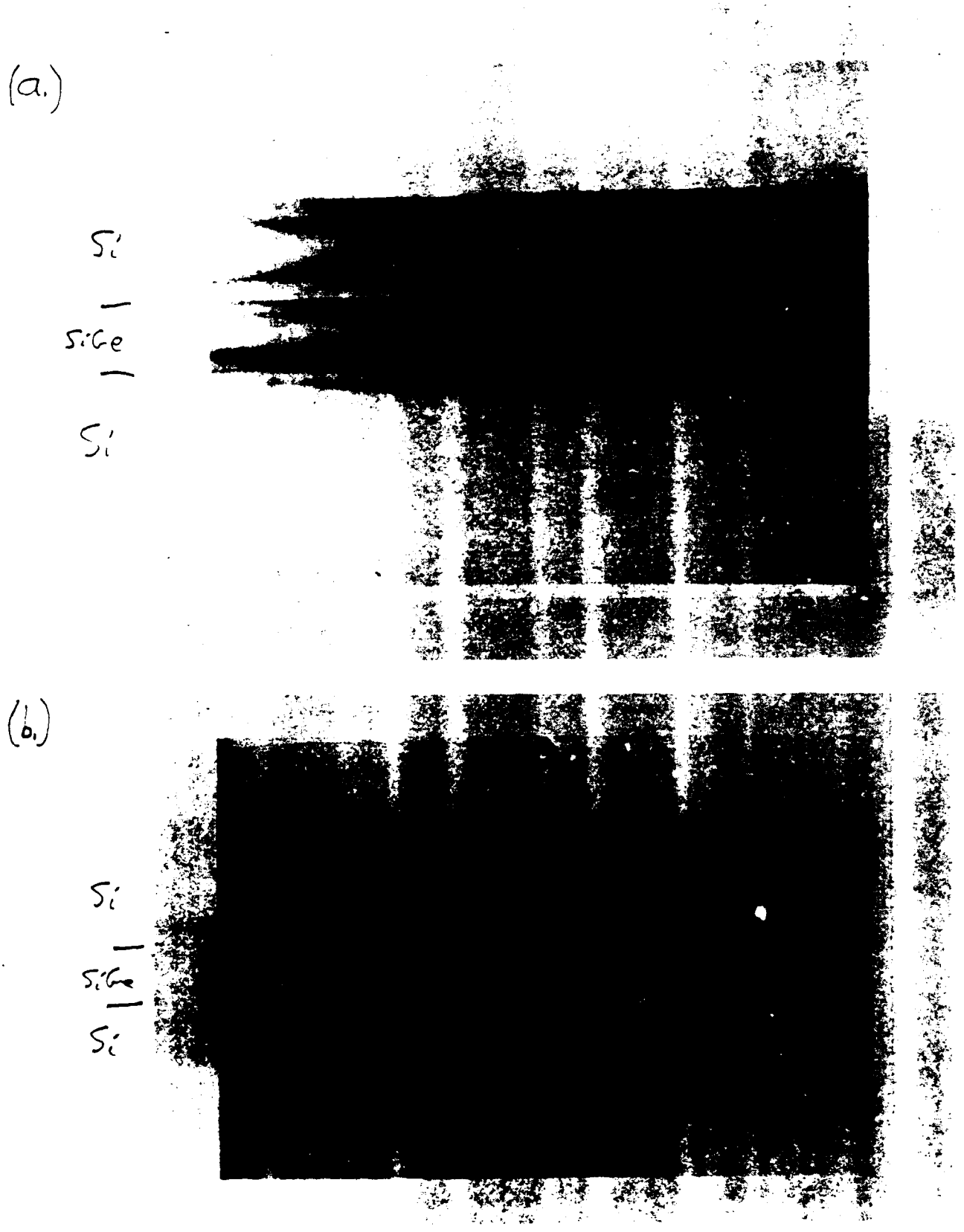

FIG. 5

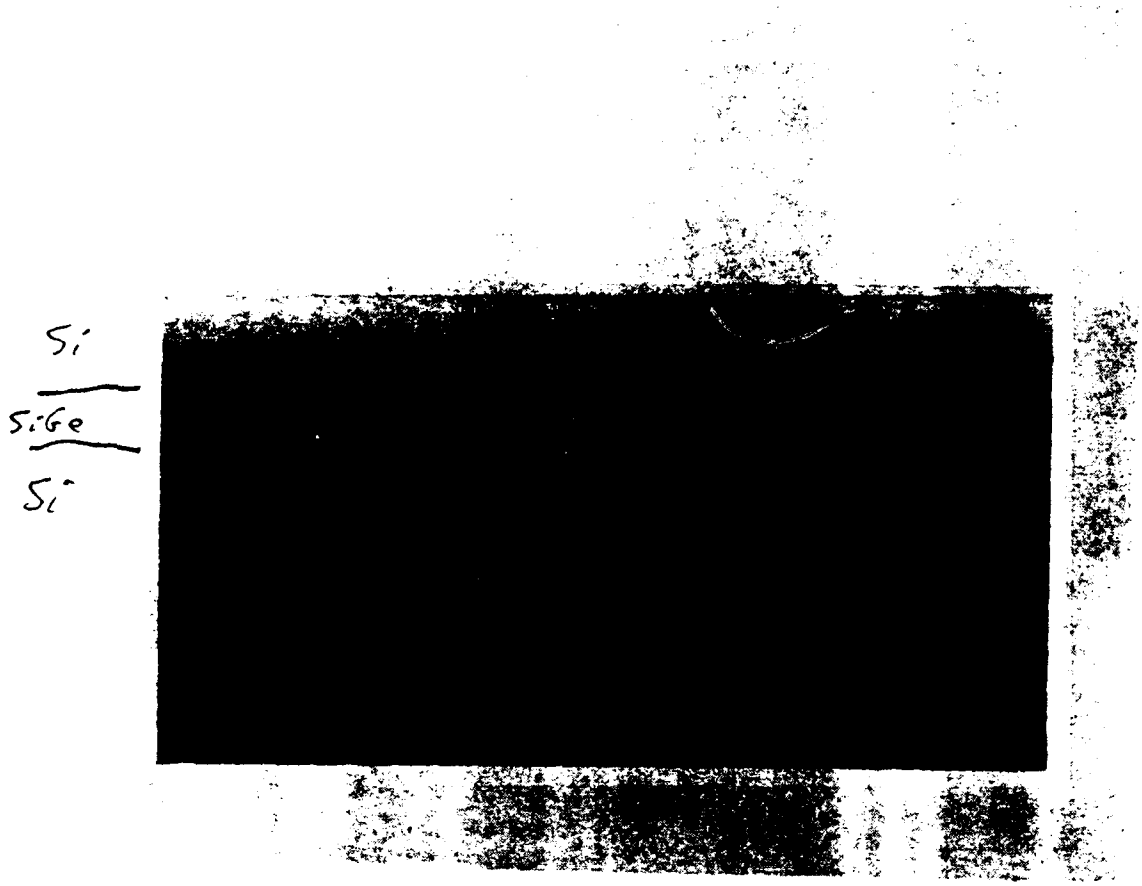

FIG. 6

Fig. (a)

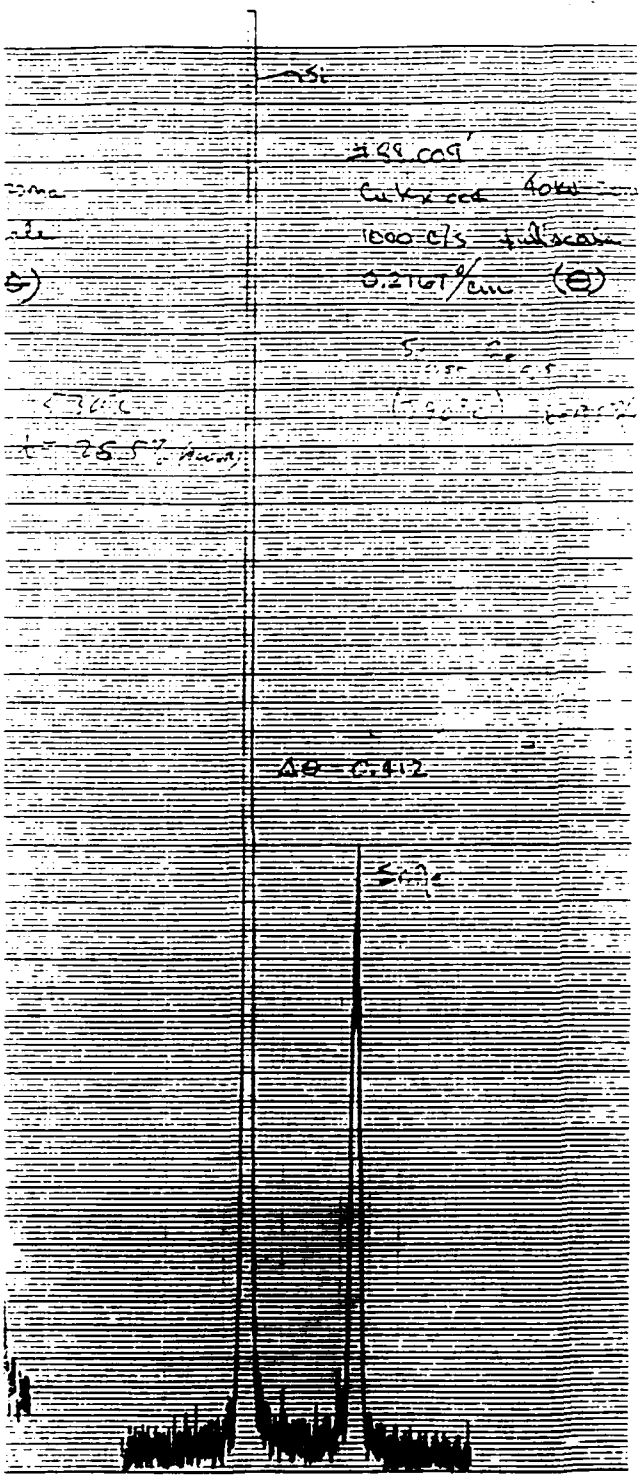

Fig. (b)

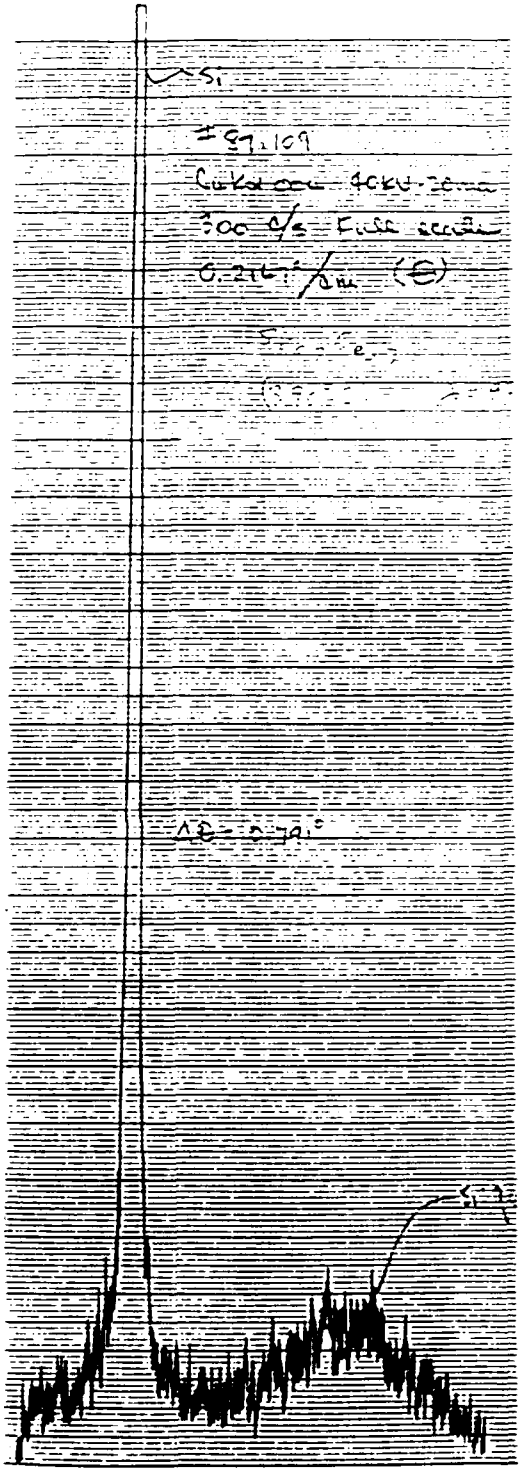

4d

FIG. 7

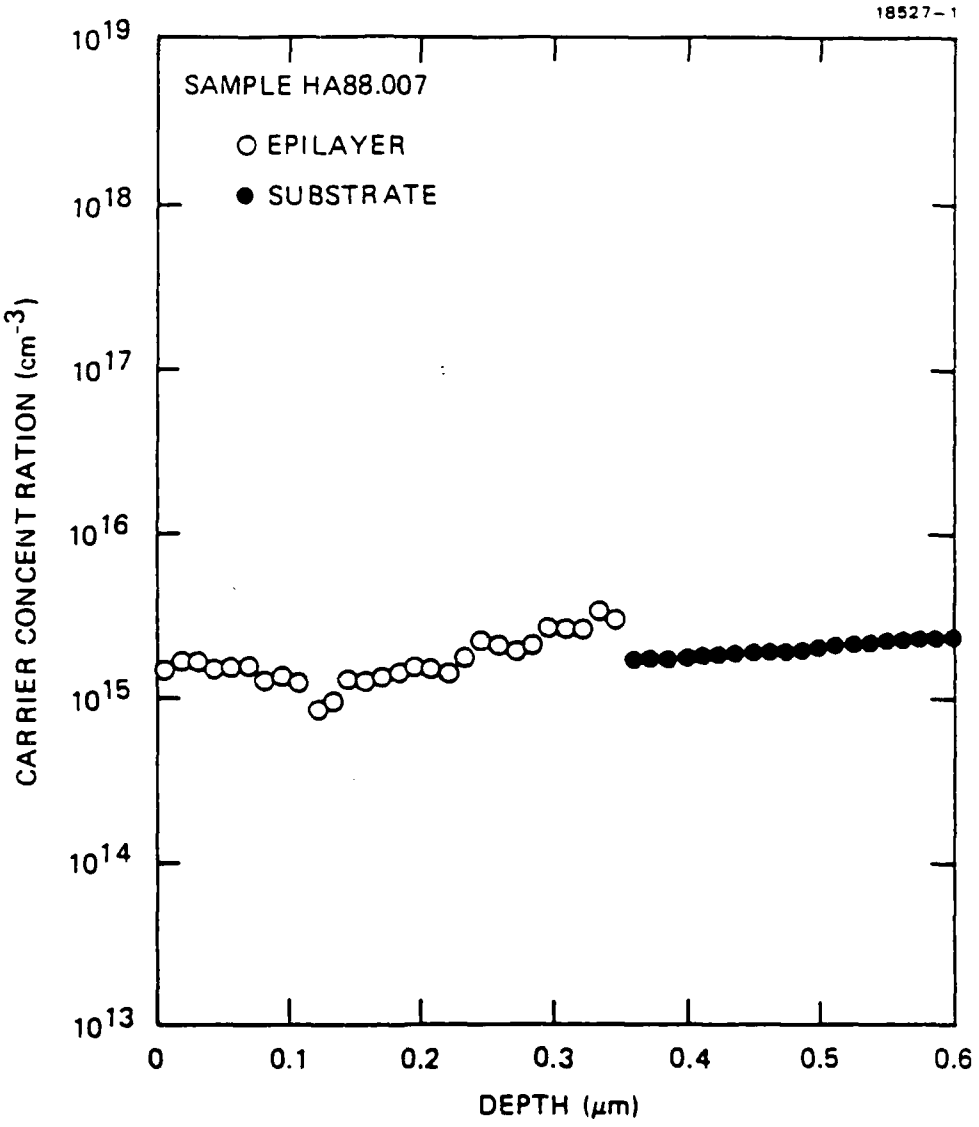

HAUSMANN

FIG. 8

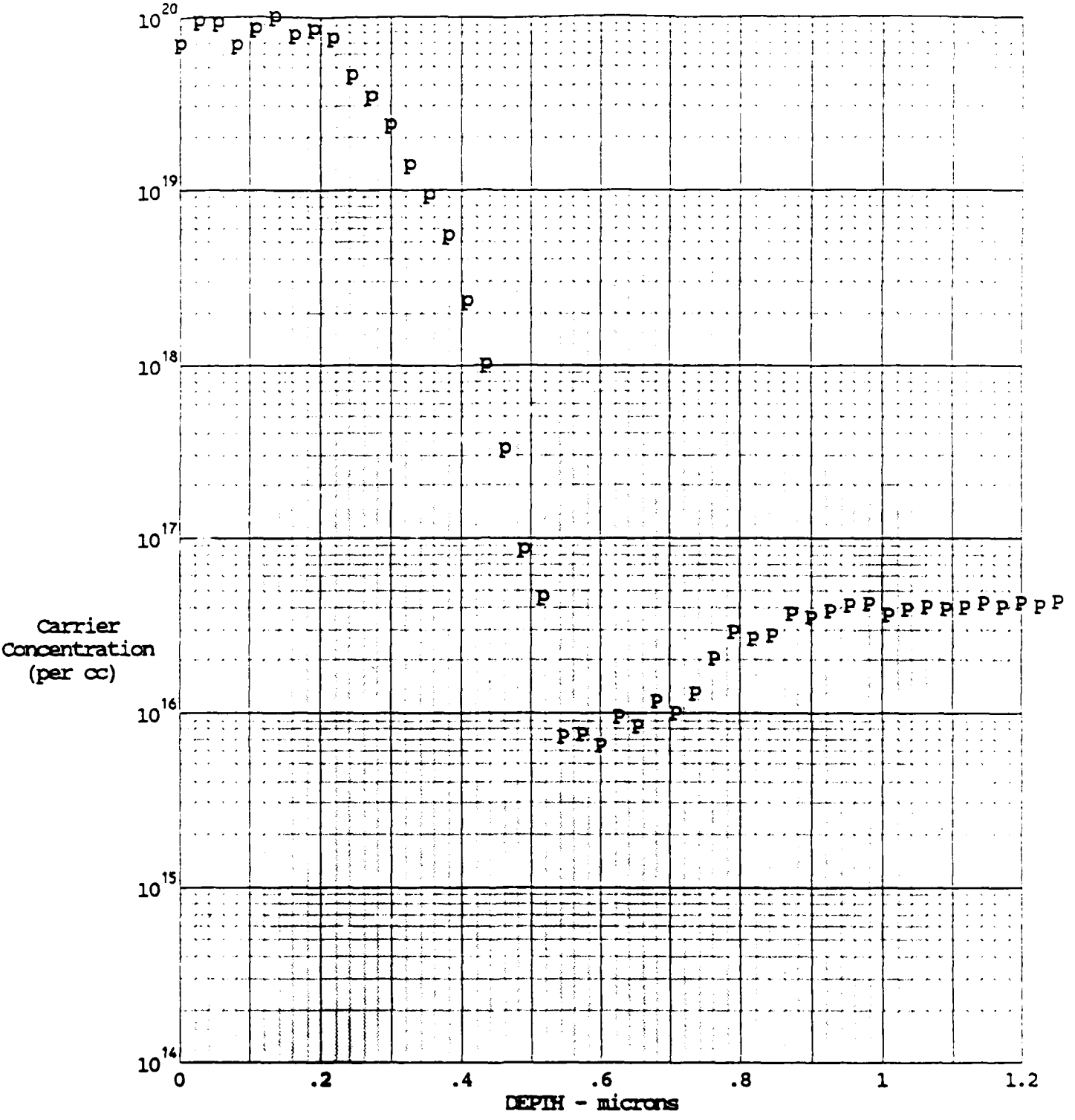

Date	09/21/88	Probe Load	5.0 g	Orientation	<100>
File #	CMBD0294	Bevel Angle	.0054		
Source	HUGHES MLB.	Step Increm	5 um	Sample #	88.035

SOLECON LABORATORIES
INCORPORATED
3001 RED HILL AVE #4-118 COSTA MESA, CA 92626 (714) 549 0203

FIG. 9